communications biology

A Nature Portfolio journal

Article

https://doi.org/10.1038/s42003-025-08360-w

# Myc overexpression improves recovery from myocardial infarction associated with cardiomyocyte hyperplasia in the mouse heart

Check for updates

Cristina Villa del Campo [1,2] ✉, Morena Raiola[1], Rocío Sierra[1], Ignacio MS[1], Jorge Peña-Peña [1], Isaac Esteban[1,3] & Miguel Torres [1,2] ✉

Adult mammalian hearts lack the ability to regenerate after a myocardial infarction, which leads to heart failure progression. Therefore, finding ways to promote regeneration is a major goal in the development of cardiovascular therapies. In this study, we focus on the role of Myc moderate overexpression in response to acute ischemic injury. We have previously shown that moderate Myc overexpression is not detrimental to cardiac function and promotes cell competition and a hyperplastic phenotype. Here, we describe that Myc overexpression in non-regenerative postnatal hearts promotes functional improvements and reduced scar formation after myocardial infarction. This response correlates with a hyperplastic phenotype in postnatal and adult hearts, characterized by bigger hearts, smaller cardiomyocyte size and increased BrdU incorporation without ploidy increase. Moreover, we show that Myc strongly enhances diploid cardiomyocyte proliferation and the generation of new binucleated cardiomyocytes. Thus, Myc promotes functional and morphological improvements in the heart following acute ischemia and this response correlates with promotion of hyperplasia versus hypertrophy.

Heart failure (HF) is a leading cause of morbidity and mortality worldwide, ultimately requiring palliative therapy or heart transplantation[1]. A primary reason for the progression of heart failure is the limited regenerative ability of the adult mammalian heart[2,3].

In mice and other mammals, there is potential to recover from ischemic cardiac damage and regenerate the heart during the first days of life[4,5]. Similarly to what has been described for zebrafish, this regeneration is driven by the proliferation of pre-existing cardiomyocytes[5,6]. Shortly after birth, cardiomyocytes shift from hyperplasic to hypertrophic growth and exit cell cycle[2,5]. This renders the cardiac tissue with a low turnover of cardiomyocytes[7] that is insufficient to compensate cardiac function after ischemic damage. Therefore, in adult mammals, cardiomyocytes that survive an ischemic episode compensate for the overload by hypertrophy and hyperploidy, frequently leading to remodeling and heart failure. The postnatal exit from the cell cycle is concomitant with an increase in ploidy, which in the mouse appears mostly in the form of binucleation and represents a barrier for cell proliferation[8–10]. For this reason, the potential proliferative ability of the adult myocardium is thought to rely on the small proportion of adult cardiomyocytes that remain diploid in mammals. This is supported by the fact that cardiomyocytes of newborn mammals and adult zebrafish are diploid, and experimental cardiomyocyte polyploidization impairs zebrafish heart regeneration[11,12].

Myc and Mycn are bHLH transcriptional activators, with Mycn being essential for fetal cardiomyocyte proliferation, and Myc able to functionally replace it[13]. Strong overexpression of Myc in adult mouse cardiomyocytes activates the cell cycle associated with pathological cardiac hypertrophy[14–19]. Conversely, Myc moderate overexpression provides cardiomyocytes a competitive advantage without inducing functional impairment, both during heart development and adult homeostasis[20]. Furthermore, Myc overexpression limits cardiac damage following ischemia-reperfusion ex vivo by regulating energy metabolism[16]. Notably, in a mouse model of Myc-ER overexpression, adult cardiomyocytes over P14 were shown to be refractory to cell cycle activity induction through Myc-ER activation by Tamoxifen, due to low levels of the limiting factor P-TEFb[14].

[1]Cardiovascular Regeneration Program, Centro Nacional de Investigaciones Cardiovasculares (CNIC), Madrid, 28029, Spain. [2]Centro de Investigación Biomédica en Red de Enfermedades Cardiovasculares (CIBERCV), Madrid, 28029, Spain. [3]Institute for Biomedical Engineering, ETH, Zurich, 8093, Switzerland.
✉e-mail: cvilla@cnic.es; mtorres@cnic.es

However, the cellular and functional effects of Myc overexpression following in vivo ischemic injury in mammalian hearts remain to be elucidated. Here, we used cardiomyocyte-specific genetic overexpression of homeostatic levels of wild-type *Myc*, to address its effect in non-regenerative neonatal and adult hearts. Upon permanent left anterior descending (LAD) artery ligation, Myc moderate overexpression led to less scarring and functional improvement. Analysis of cardiomyocyte biology showed a hyperplastic response with increased DNA synthesis both in the mononuclear and binuclear populations and a reduction in cardiomyocyte size. Our findings show that Myc overexpression activates the cell cycle and prevents hypertrophy of postnatal mammalian cardiomyocytes, which associates with an improved mammalian heart's response to acute ischemic injury.

## Results and discussion

### Myc overexpression promotes cardiomyocyte cell cycle activity with no increase in ploidy and preservation of cardiac function

To investigate the effect of Myc in non-regenerative mouse hearts, we used conditional overexpression of wild-type *Myc* driven by the endogenous *ROSA26* promoter[21] by inducing recombination of a *Rosa26* knock-in allele in cardiomyocytes using MHC-Cre[22] (Table 1). We have previously described that this genetic model produces stable, homeostatic levels of Myc overexpression without altering heart function[20]. Here we studied the consequences of increasing Myc dose using one or two alleles of *Myc* overexpression from the *Rosa26* locus. Assessment of postnatal day 28 (P28) hearts showed no histological alteration (Fig. 1A), and uncompromised heart function following activation of two *Rosa26-Myc* alleles (Fig. 1B), although a moderate increase in heart to body weight ratio was observed in hearts overexpressing 1 or 2 *Myc* copies (Fig. 1C).

To understand the mechanism driving the increase in heart size, we studied the effect of Myc overexpression on cell cycle activity in homeostatic conditions. Assessment of proliferation in P1 neonatal cardiomyocytes showed a 5-fold increase in phosphorylated histone H3 (PH3) in *Myc*-overexpressing cardiomyocytes (Fig. 1D). Additionally, BrdU administration to adult mice over a 3-week period revealed a significant rise in cell cycle activity, in both mononucleated and binucleated cardiomyocytes (Fig. 1E). To determine whether this increase in DNA synthesis in adult cardiomyocytes produced changes in ploidy, we determined nuclear volume, which is a surrogate measure for DNA content[23]. In both bi- and mononucleated cardiomyocytes we observed no significant changes in nuclear volume, with a tendency to decrease in both populations of Myc-overexpressing hearts (Fig. 1F). These results indicate that the increase in DNA synthesis induced in bi-nuclear cardiomyocytes by Myc overexpression does not induce polyploidization. Moreover, they indicate that the increase in DNA synthesis induced in mononuclear cardiomyocytes by Myc overexpression (Fig. 1E) is due to the stimulation of diploid cardiomyocyte proliferation and not to polyploidization.

### Myc overexpression reduces myocardial damage and improves cardiac function in non-regenerative postnatal mice

Next, we sought to determine the effect of Myc overexpression on acute ischemic injury in non-regenerative conditions. We performed permanent LAD artery ligation in postnatal day 7 mice (P7), analyzing heart function via echocardiography and scar formation 21 days post-injury (P28). Hearts with Myc overexpression showed smaller scar size 21 days post-injury (Fig. 2A, B), correlating with functional improvement (Fig. 2C), and increased heart-to-body weight ratio (Fig. 2D).

### Myc-overexpressing hearts display a reduced cardiomyocyte hypertrophy that is maintained after ischemic injury

Prior studies described strong Myc overexpression to drive cardiomyocyte hypertrophy[24]. To further clarify the effects of moderate *Myc* overexpression, we analyzed cardiomyocyte size by cross-sectional area measurement in histological sections. Contrary to previous studies, we found a reduction in cardiomyocyte size in P28 uninjured hearts (Fig. 2E top, F left), mirroring what we previously reported in hearts that overexpress Myc from a single *Rosa26-Myc* allele[20]. Cardiomyocyte size analysis in P28 mice after LAD artery ligation at P7 showed a shift towards higher cross-sectional area in WT hearts, indicating a cardiomyocyte hypertrophic response (Fig. 2E, bottom left, F right). Cardiomyocyte from hearts with 1 or 2 additional doses of Myc also showed an increase in size post LAD, however, they remained less hypertrophic than cardiomyocytes of control hearts (Fig. 2E bottom, F right). These findings, along an increased organ size (Figs. 1C, 2D), suggest that Myc moderate overexpression induces a cardiac hyperplastic response while reducing cardiomyocyte size in uninjured hearts, and limiting hypetrorphy associated with the response to ischemic injury.

### Myc overexpression reduces myocardial damage and limits cardiomyocyte hypertrophy in adult mice

Acute ischemic injury by LAD ligation in adult (8–12 week) mice showed similar, albeit milder effects than in P7 mice (Fig. 3). Scar size was reduced significantly (Fig. 3A, D), whereas ejection fraction exhibited a positive trend in Myc-overexpressing hearts (Fig. 3B). The heart-to-body weight ratio showed a non-significant trend to increase (3C). Similarly to P7 injured hearts, overexpression of Myc blunted the cardiomyocyte hypertrophic response after injury in adult hearts; evidenced by smaller cardiomyocyte cross-sectional area (Fig. 3E).

### Myc overexpression activates mononuclear cardiomyocytes for self-renewal and generation of new binucleated cardiomyocytes in injured hearts

Cardiomyocyte nucleation significantly influences the heart's response to acute ischemia and correlates with cardiomyocyte size[11,12]. Thus, we examined whether Myc overexpression affected cardiomyocyte populations regarding their nuclei number. Myc overexpression in uninjured hearts increased the proportion of mononucleated cardiomyocytes, whereas binucleated or multinucleated cardiomyocyte populations remained unchanged (Fig. 4A–C left). These observations agree with the increased BrdU incorporation in cardiomyocytes of adult Myc-overexpressing hearts (Fig. 1E). This increase in mononucleated cardiomyocytes lost significance in post-MI hearts; however, in this case we observed a significant decrease in the proportion of binucleated cardiomyocytes (Fig. 4A-C right). The population of cardiomyocytes with more than two nuclei was unaffected by Myc overexpression, but both, WT and Myc overexpressing hearts, showed increased proportions following MI (Fig. 4C), which correlates with the increase in cardiomyocyte size following LAD (Fig. 3F). These results indicate that inhibition of cardiomyocyte hypertrophy by Myc involves changes in cardiomyocyte nucleation, in both homeostatic and injured hearts.

Next, to study cardiomyocyte renewal, we determined DNA synthesis in the hyperplastic response induced by Myc overexpression. BrdU was administered for 21 days following LAD ligation at P7 and in age-matched uninjured controls. Incorporation was detected in all cardiomyocyte populations (mononuclear, binuclear and multinuclear) (Fig. 4D). In uninjured hearts, Myc overexpression led to a mild increase in BrdU incorporation exclusively in the mononucleated cardiomyocyte population (Fig. 4E left), which matches the higher proportion of mononuclear cardiomyocytes in Myc-overexpressing hearts (Fig. 4A) as well as their ploidy (Fig. 1G). In post-MI hearts, a strong increase in BrdU incorporation was detected in mononucleated cardiomyocytes of both control and Myc-overexpressing hearts, without significant differences between the two genotypes (Fig. 4E right). Control binucleated cardiomyocytes showed a moderate increase in BrdU incorporation (1.6x relative to this population in uninjured hearts) and multinucleated cardiomyocytes showed no differences after MI. In contrast, a marked increase in DNA synthesis was observed in binucleated (3.6x) and multinucleated cardiomyocytes (2.7x) in Myc-overexpressing hearts (Fig. 4E). Notably, the proportion of binucleated cardiomyocytes incorporating BrdU doubled in Myc-overexpressing versus WT hearts, reaching 14% of the total binucleated cardiomyocyte population (Fig. 4E). Given the different predominance of cardiomyocyte populations,

**Table 1 | Summary of reagents used in this manuscript**

| Reagent/resource | Reference or Source | Identifier or Catalog number |
|---|---|---|
| *Experimental models* | | |
| iMOS-Myc | Claveria, C 2013 | NA |
| MHC-Cre | Agah, R 1997 | NA |
| *Antibodies* | | |
| Rat monoclonal [BU1/75 (ICR1)] to BrdU - Proliferation Marker | Abcam | ab6326 |
| Mouse monoclonal [EA-53] to Sarcomeric Alpha Actinin | Abcam (Netherlands) B.V. | ab9465 |
| Rabbit monoclonal PH3 antibody | PTM Bio | PTMPTM-1001RM-100 |
| Goat anti-Rat IgG (H + L) Highly Cross-Adsorbed Secondary Antibody, Alexa Fluor™ Plus 488 | Thermo Fisher | A48262 |
| DAPI (4',6-diamidino-2-fenilindol, dihidrochloride) | Thermo Fisher | D1306 |
| Wheat germ agglutinin-Alexa Fluor 647 | Thermo Fisher | W32466 |
| *Chemicals, Enzymes and other reagents* | | |
| H&E | | |
| Masson Trichrome | | |
| 5-BROMO-2'-DEOXYURIDINE | Merck Life Science, S.L.U. | B5002-5G |
| DNASE I RECOMBINANT, RNASE-FREE SOLUTION | Merck | 4716728001 |
| Sodium chloride | Sigma-Aldrich | S9625-500G |
| Potassium choride | Sigma-Aldrich | P4504-500G |
| Potassium phosphate monobasic | Sigma-Aldrich | P5379-100G |
| Sodium phosohate dibasic | Sigma-Aldrich | S0876-100G |
| Magnesium sulfate heptahydrate | thermoscientific | 423900250-25 g |
| Sodium bicarbonate | Sigma-Aldrich | S5761-500G |
| Potassium bicarbonate | Sigma-Aldrich | 431583-50 G |
| Taurine | Sigma-Aldrich | T0625-100G |
| Butanodione monoxime (BDM) | Sigma-Aldrich | T0625-10g |
| Glucose | Sigma-Aldrich | B0753-25G |
| Liberase TM 100 mg | Roche Appl. Biosc | G7528-250G |
| Trypsin 2,5% | Gibco | 5401127001 |
| HEPES salt | Sigma-Aldrich | H3375-25G |
| 400u-Dish 35 mm high ibiTreat | Ibidi | 81156-400 |
| Neonatal Heart Dissociation Kit, m&r | Miltenyi Biotec S.L. | 130-098-373 |
| Laminin Mouse Natural 1 mg | Cultek, S.L.U. | 354232 |
| Formaldehyde 4% aqueous solution, bufferes | VWR CHEMICALS | 12051-08 |
| *Software* | | |
| Fiji-imageJ | http://rsb.info.nih.gov/ij | RRID:SCR_002285 |
| Prism 9 | GraphPad | |
| *Other* | | |
| VEVO 2100 | Visual Sonics | |
| Digitalizador | Hamamatsu Nanozoomer 2.0 | |
| Nikon A1R | Nikon | |

we calculated the proportion of BrdU+ cardiomyocytes of different nuclei number relative to the total cardiomyocyte population (Fig. 4F). This graph shows that 16,4% of Myc-overexpressing cardiomyocytes underwent DNA synthesis after injury, compared to 8,5% in control hearts. Remarkably, the binucleated population alone contributes 73% of the total population of cardiomyocytes that incorporated BrdU in Myc-overexpressing hearts.

In this study, we show that Myc induces a heart repair response when overexpressed in cardiomyocytes at moderate levels. Contrary to previous findings[14–19], we observed no functional impairment or histological alterations induced by Myc overexpression in homeostatic conditions. Moreover, Myc-overexpressing hearts displayed higher cell cycle activity in basal conditions, both in neonatal and adult hearts, alongside a higher proportion of mononuclear cardiomyocytes. Following permanent LAD ligation, these hearts exhibited improved morphological and functional recovery, characterized by smaller infarct size and improved cardiac function. This is at least partly mediated by the hyperplastic features of these hearts: larger organ size, with smaller cardiomyocytes and higher cell cycle activity in homeostatic conditions. These results contrast with previous models of Myc overexpression in the heart, which showed a hypertrophic response upon Myc overexpression. However, while here we used levels of wild type Myc overexpression within a physiological range[20], prior results in the field used Myc versions fused to the Estrogen Receptor Ligand Binding Domain and/or non-physiological levels of overexpression[14–19]. Interestingly, this effect of Myc overexpression persisted in damaged hearts, as we observed that following MI, Myc overexpression limited the extent of cardiomyocyte hypertrophy.

It is well-established that heart regeneration, in both mammals and ZF, relies on the proliferation of pre-existing diploid cardiomyocytes[5,6]. Additionally, the proportion of mononuclear cardiomyocytes has been correlated with cardiac regenerative ability[10]. In our study, Myc overexpression significantly increased the number of mononuclear cardiomyocytes in uninjured hearts and increased heart size but reduced cardiomyocyte size. These results suggest that Myc overexpression promotes cardiomyocyte proliferation in uninjured hearts. Following acute myocardial infarction, the greater DNA synthesis detected in Myc-overexpressing hearts compared to controls suggests increased cardiomyocyte proliferation. Although increased DNA synthesis could relate to cardiomyocyte hypertrophy rather than proliferation, the smaller cardiomyocyte size and the higher proportion of mononuclear cardiomyocytes in Myc-overexpressing hearts strongly suggests that much of this DNA synthesis is dedicated to proliferation. Notably, following injury, Myc overexpressing hearts show the highest BrdU incorporation rates in binucleated cardiomyocytes. The pool of BrdU-positive cardiomyocytes is unlikely to originate from pre-existing binucleated cardiomyocytes as they are rarely proliferative[8]. Hence, the most plausible explanation for this increase is that they arise from mononuclear cardiomyocytes undergoing binucleation. This mechanism would explain why post-MI, the abundance of mononuclear cardiomyocytes is relatively reduced in Myc-overexpressing hearts (Fig. 4A), despite similar BrdU incorporation proportions observed in both genotypes (Fig. 4E). Our experiments thus reveal the ability of mononuclear diploid cardiomyocytes to generate new binucleated cardiomyocytes. This generation of new binucleated cardiomyocytes from pre-existing mononuclear ones is activated following acute ischemia and is strongly enhanced by Myc overexpression. This mechanism recapitulates postnatal development, when mononuclear cardiomyocytes undergo binucleation to produce fully differentiated cardiomyocytes that can meet the contractile demands of the postnatal heart. Therefore, we propose a model in which Myc overexpression enhances this pathway both by stimulating self-renewal of mononuclear cardiomyocytes and by promoting the generation of a substantial fraction of new binucleated cardiomyocytes. Given that an excess of mononuclear immature cardiomyocytes leads to cardiac insufficiency, we suggest that Myc's ability to induce the production of new binucleated cardiomyocytes underlies its beneficial effects on heart function following myocardial infarction.

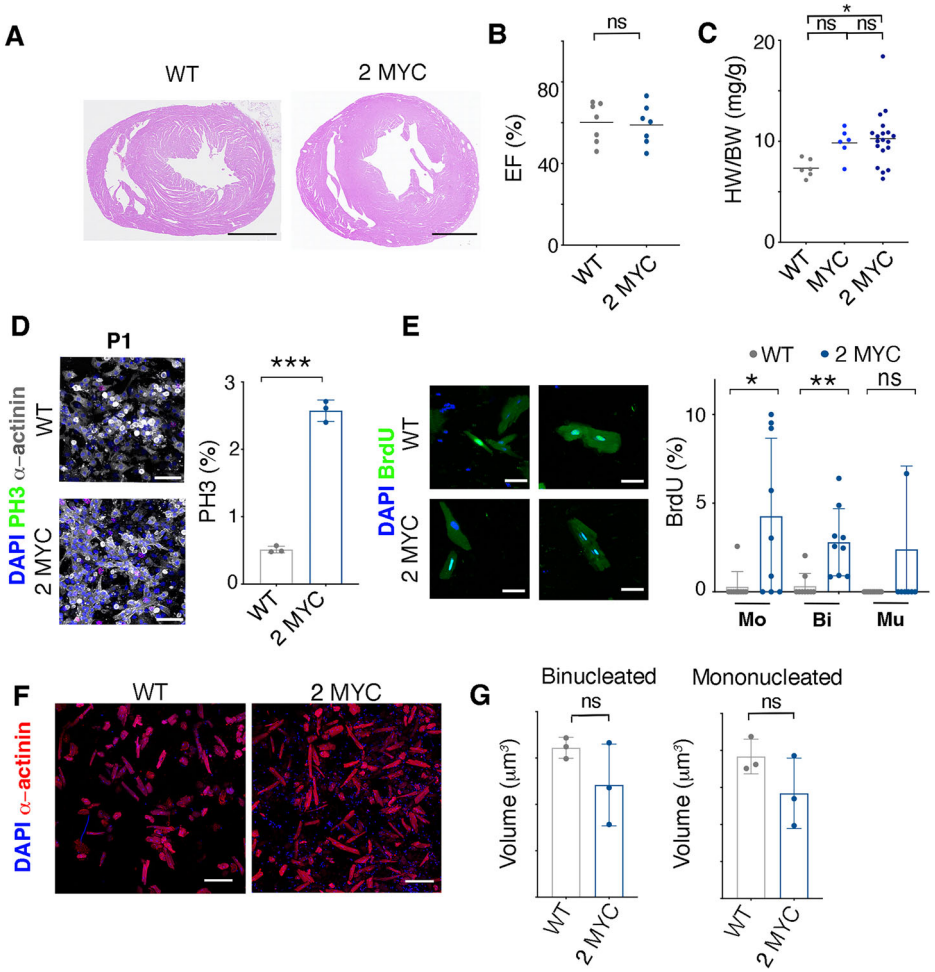



**Fig. 1 | Moderate Myc overexpression in postnatal cardiomyocytes is phenotypically silent in homeostasis and promotes cardiomyocyte cell cycle activity with no increase in ploidy. A** Histological heart sections stained with hematoxylin/eosin of WT mice and mice overexpressing two alleles of Myc (2MYC) at 28 days. **B** Percent EF at 28 days of age. **C** Heart to body weight ratio (mg/g) at 28 days. Data are presented as individual hearts and mean. **D** Representative confocal images of isolated P1 cardiomyocytes stained for α-actinin and PH3 for WT and MYC overexpressing hearts (left). Percent of PH3 positive cardiomyocytes. **E** Representative confocal images of adult isolated cardiomyocytes stained for BrdU (left). BrdU+ cardiomyocyte proportion in each cardiomyocyte population in uninjured adult hearts (10–12 weeks) (right). (Mo: mononucleated, Bi: binucleated, Mu: Multinucleated). **F** Representative confocal images of isolated adult cardiomyocytes stained for actinin and DAPI for nuclear volume segmentation. **G** Average nuclear volume per heart shown in $\mu m^3$ for WT and Myc-overexpressing hearts in mononucleated and binucleated cardiomyocytes ($n > 300$ nuclei/heart). Data presented as individual hearts, mean and error bars (when shown) represent SD. Scale bars: 1 mm in A; 70 μm in (**D**); 60 μm in (**E**); 200 μm in (**F**). $^{*}p < 0.05$ $^{**}p < 0.01$ $^{***}p < 0.001$ $^{****}p < 0.0005$.

In conclusion, we report that moderate overexpression of WT Myc in cardiomyocytes promotes a beneficial response after ischemic injury in mouse hearts, associated with cardiomyocyte hyperplasia versus hypertrophy and stimulation of the generation of new binucleated cardiomyocytes.

## Methods

### Mouse Strains

All experiments were performed using mice (Mus musculus) of a mixed background that were maintained and handled according to the recommendations of the CNIC Ethics Committee, the Spanish laws and the EU Directive 2010/63/EU for the use of animals in research. We have complied with all relevant ethical regulations for animal use. The experimental protocols involving animals were approved by the CNIC and Universidad Autónoma de Madrid Committees for "Ética y Bienestar Animal" and the area of "Protección Animal" of the Comunidad de Madrid with reference PROEX 220/15.

*iMOS* Mouse lines have been previously described[21]. Homozygous *iMOS* females were mated with Homozygous *iMOS* males carrying MHC-Cre lines[22] Mice were aged-matched P7 in neonatal surgery and 8–12 weeks in adults. Mice sex was not biased and matched between experimental groups. No differences were observed between sexes. Mice were euthanized using cervical dislocation.

BrdU 0.5 mg/ml was administered to adult mice through the drinking water for one month.

### Echocardiographic functional examination in mice

Echocardiographic evaluations to determine cardiac volume and LV contractility were performed by an experienced observer blinded to the study allocation in mice at 21 days post-infarction. Mice were anesthetized by inhalation of isoflurane/oxygen and examined with a 30-MHz transthoracic echocardiography probe and a Vevo 2100 ultrasound system (VisualSonics, Toronto, Canada). From short-axis and long-axis B-mode views, end-systolic and end-diastolic LV volumes and LV ejection fraction (LVEF) were calculated using the area-length method[25].

### Neonatal cardiomyocyte isolation

P1 cardiomyocytes were isolated using Mylteni isolation kit and following the manufacturers' directions.

### Neonatal myocardial infarction by permanent LAD ligation

Neonatal P7 mice used in MI experiments were anaesthetized using hypothermia. Neonates (P7) were exposed to hypothermia for 180 s. MI was performed by permanent ligation of the left anterior descending coronary artery. After lateral thoracotomy is performed, an 8-0 suture is used to ligate the LAD. At final timepoint (21 days post injury), heart function was monitored by echocardiography, animals were sacrificed, hearts dissected and processed for histological analysis or cardiomyocyte isolation.

### Adult myocardial infarction by permanent LAD ligation

For permanent myocardial infarction, we subjected 8- to 12-week-old male mice to permanent occlusion of the left anterior descending (LAD) coronary artery to measure long-term cardiac function. Cardiac function was measured at basal time and days 15, 30, 45 and 60 post occlusion by echocardiography. At final timepoint, animals were sacrificed, hearts dissected and processed for histological analysis.

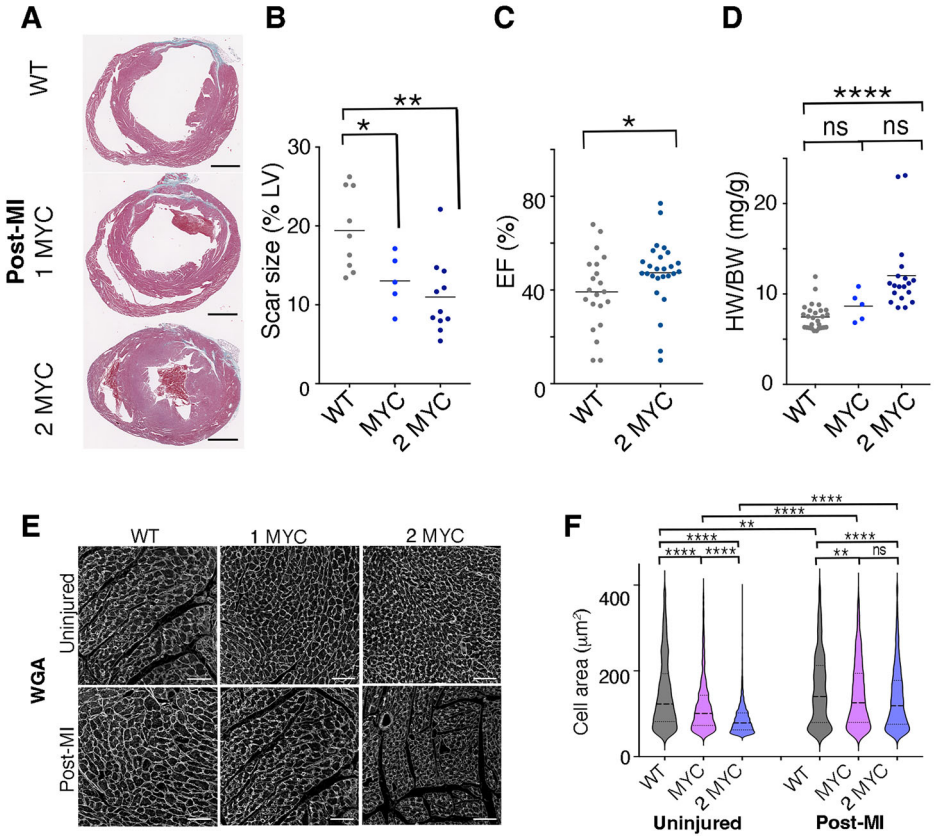



**Fig. 2 | Moderate Myc overexpression promotes a repair response after ischemic injury involving hyperplasia of the cardiomyocyte population.** **A** Histological sections stained with Masson's trichrome showing scarring (blue) and healthy muscle (pink) after ischemic injury performed at P7 and analyzed 21 days after surgery (P28). **B** Scar size quantification as % of LV area 21 days post ischemic injury. **C** Percent EF 21 days post injury at P7(P28). **D** Heart weight to body weight ratio 21 days post ischemic injury at P7(P28). **E** Histological sections stained with wheat germ agglutinin (WGA-gray) of P28 non-infarcted hearts (Control) and post ischemic injury hearts at 21 days after the LAD at P7 (P28) (Post-MI) in wild type (WT) and Myc overexpressing mice (1MYC and 2 MYC). **F** Quantification of cardiomyocyte cross-sectional area distribution in P28 non-infarcted (Uninjured) and 21 days post injury (Post-MI) wild type (WT) and Myc-overexpressing (1MYC and 2 MYC) hearts. Data presented in B as distribution of individual cardiomyocyte area ($n > 1000$ cells/condition) and mean. Data presented as individual hearts and mean. Scale bars: 50 µm. $^{*}p < 0.05$ $^{**}p < 0.01$ $^{***}p < 0.001$ $^{****}p < 0.0005$.

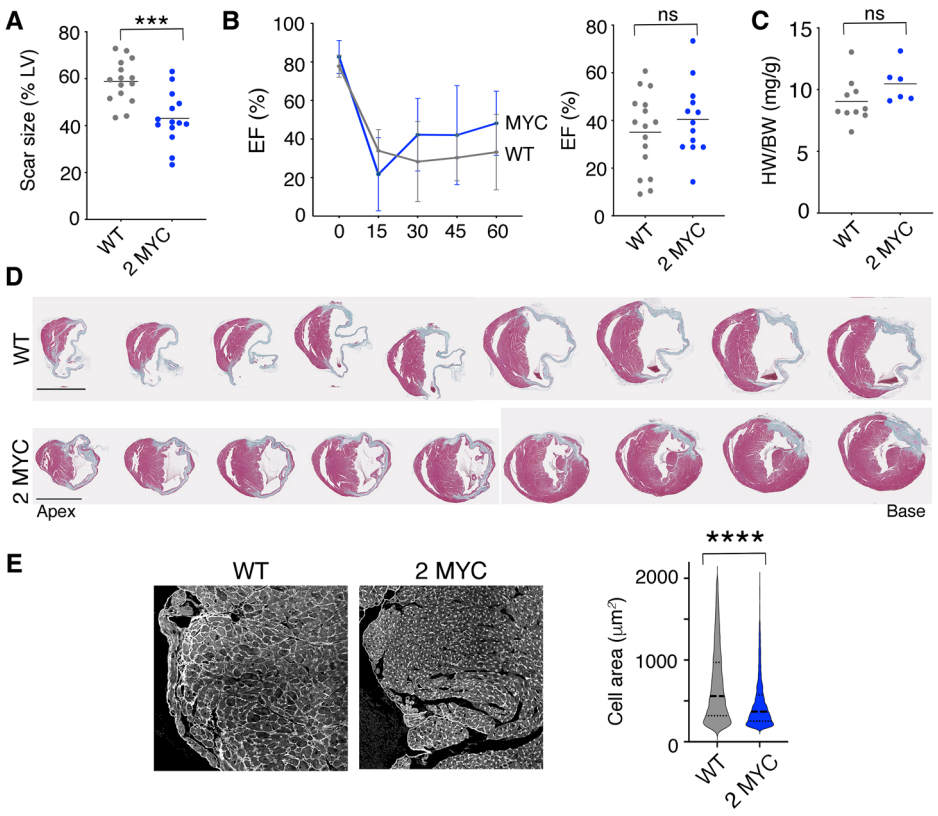



**Fig. 3 | Myc mild overexpression promotes a regenerative response with no hypertrophy in adult hearts following ischemic injury.** **A** Scar size as % of LV 60 days post ischemic injury. **B** Left: Percent EF post ischemic injury in adult mice showing evolution over time (days). Right: Percent EF 60 days post ischemic injury in adult mice (final time point). **C** Heart weight-to-body weight ratio 60 days post ischemic injury. **D** Histological sections stained with Masson's Trichrome showing scarring 60 days post ischemic injury from apex to base in WT and Myc overexpressing (2MYC) hearts. **E** Histological sections of hearts stained with wheat germ agglutinin (WGA-gray) post ischemic injury 60 days after LAD in wild type (WT) and Myc overexpressing hearts (1MYC and 2 MYC) (left). Quantification of cardiomyocyte cross-sectional area distribution post ischemic injury 60 days after LAD ligation in wild type (WT) and Myc-overexpressing hearts (2 MYC) (right). Data presented as individual hearts, mean and error bars (when shown) represent SD. Data presented in (**E**) as distribution of individual cardiomyocyte area ($n > 1000$ cells/condition) and mean. Scale bars: 2 mm. $^{*}p < 0.05$ $^{**}p < 0.01$ $^{***}p < 0.001$ $^{****}p < 0.0005$.

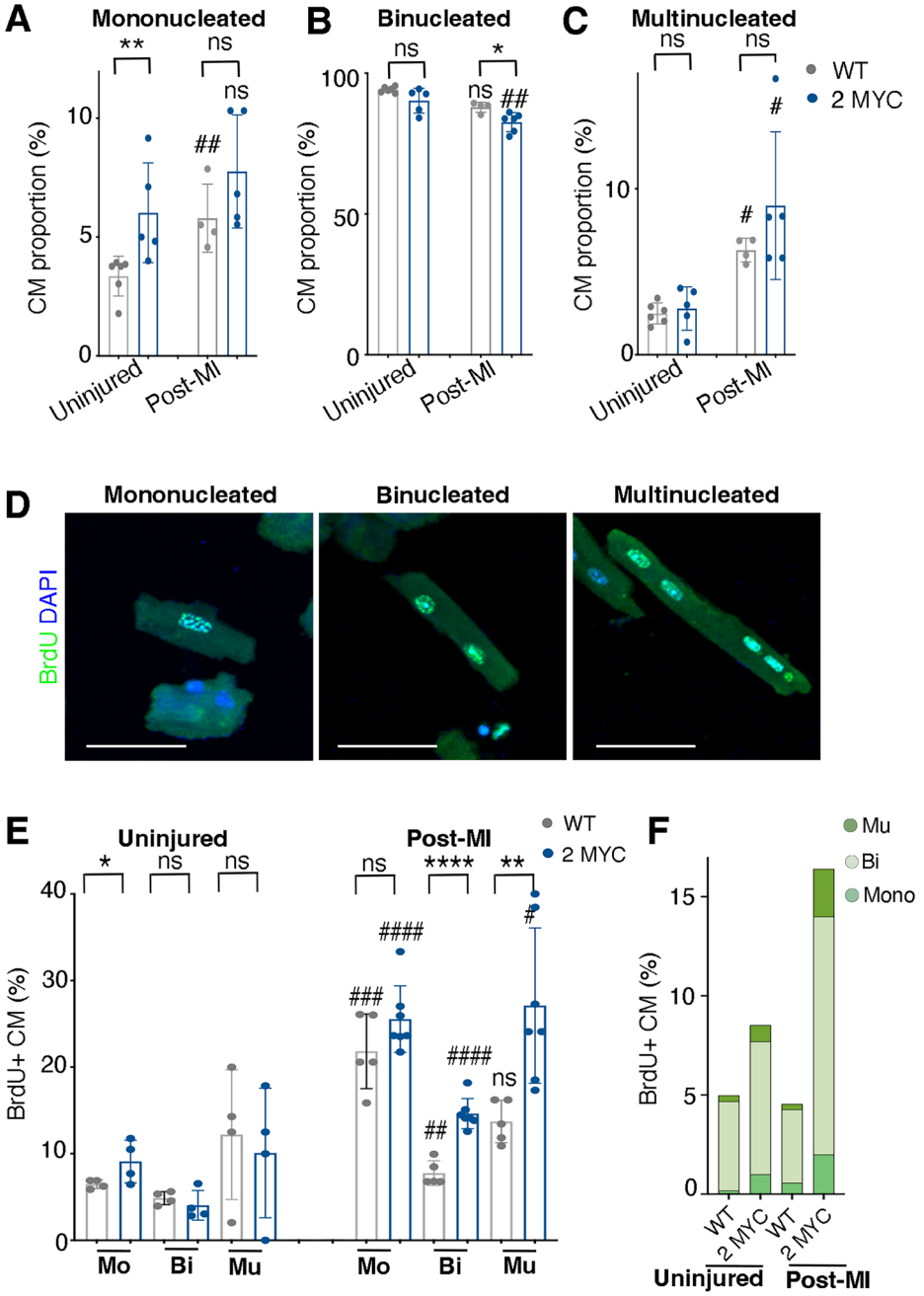



**Fig. 4 | Myc mild overexpression promotes no major alteration in cardiomyocyte populations and activates cell cycle in cardiomyocytes after ischemic injury. A–C** Quantification of cardiomyocyte population proportions in P28 uninjured hearts (Uninjured) and hearts that suffered ischemic injury at P7 analyzed at P28 (Post-MI) for mononucleated (**A**), binucleated (**B**) and multinucleated (**C**) CMs in WT or Myc-overexpressing hearts. **D** Representative confocal images of mononucleated, binucleated and multinucleated cardiomyocytes isolated by Langendorff digestion positively stained for BrdU (Green) and DAPI (blue). **E** Percentage of BrdU+ cardiomyocytes according to nucleation in uninjured hearts at P28 (uninjured) and hearts analyzed 21 days post ischemic injury at P7 (P28) (Post-MI) from WT and Myc-overexpressing mice. **F** Percentage of BrdU+ cardiomyocytes with respect to the total cardiomyocyte population in uninjured hearts at P28 (uninjured) and hearts analyzed 21 days post ischemic injury at P7 (P28) (Post-MI) from WT and Myc-overexpressing hearts. (Mo: mononucleated, Bi: binucleated, Mu: Multinucleated). Data presented as individual hearts, mean and error bars (when shown) represent SD. ($n$ = 500–1000 CM scored/heart). Scale bars: 50 µm *$p < 0.05$ **$p < 0.01$ ***$p < 0.001$ ****$p < 0.0005$ (* represents $p$-value when comparing WT and MYC for each condition and # represents $p$-value when comparing each genotype with its own value in control and Post-MI conditions).

### Cardiomyocyte isolation by Langendorff digestion

28-day-old iMOS-MYC or WT littermates (WT for MHC-Cre) were euthanized. The heart was quickly removed, cannulated through the ascending aorta, and mounted on a modified Langendorff perfusion apparatus. The heart was then retrogradely perfused for 7 min at room temperature (RT) with pre-filtered Perfusion-Buffer (NaCl, KCl, $KH_2PO_4$, $Na_2HPO_4$, $MgSO_4{\cdot}7H_2O$, $NaHCO_3$, $KHCO_3$, HEPES-Na salt, taurine, glucose, 2,3-butanedione-monoxime; pH 7.4). Enzymatic digestion was performed with digestion buffer (perfusion buffer with Liberase, Trypsin 2.5%) for 20 min at 37 °C. At the end of enzymatic digestion, both ventricles were isolated and gently disaggregated in Digestion Buffer. The resulting cell suspension was filtered through a 100-µm sterile mesh and transferred for enzymatic inactivation. Cells were resuspended and allowed to decant for 10 min contributing to the purification of the cardiomyocyte suspension. Cells were plated in single drops onto IBIDI plates precoated with mouse laminin for 1 h. After 1 h cells were fixed in PFA2% overnight at 4 degrees for further immunostaining.

### Heart collection and histological processing

On Day 21 after MI, hearts were harvested and processed for paraffin embedding, cut into Superfrost slides, and deparaffinized using standard methods. For H&E and Masson's trichrome staining, sections were stained according to the manufacturer's instructions. Sections were digitalized using a Hamamatsu Nanozoomer scanner.

### Fluorescence immunostaining and imaging

Histological sections were deparaffinized and incubated for 1 h with DAPI (1/2000) and 647-WGA (1/200). Isolated cardiomyocytes were stained for BrdU incorporation. Cells were treated with DNAseI (1/40 in commercial buffer) for 1 h at 37 °C and blocked with goat serum. Primary antibodies against BrdU (1/200), α-actinin (1/200) and PH3 (1/100) were incubated overnight at 4 °C. On the following day, cells were washed and DAPI (1/2000) and secondary antibody (1/500) incubation was done for 45 min to 1 h at room temperature. Histological sections and isolated cells were imaged with a Nikon A1R confocal

microscope using 405, 488 and 633 nm wavelengths and 20x/0.75 dry and 40/1.30 oil objectives.

### Image analysis

Scar area. For scar area measurements, Masson Trichrome-stained sections from apex to suture were analyzed every 100 µm. (7-8/heart) Collagen area was measured and shown in reference to the area of the LV. All measurements for a given animal were averaged.

CM area in sections. Cross-sectional area of cardiomyoctes was analyzed in sections using WGA staining. The cell membrane is detected using "Find Maxima" and "Analyze particles" in Fiji.

### All experiments were performed blindly

Volumetric nuclear measurements for ploidy determination. Confocal Z-stack images from isolated cardiomyocytes stained with DAPI were processed used Phyton language as follows: Preprocessing: Background removal using an OTSU thresholding over the image TopHat; intensity calibration across the *z*-axis using a scale factor assessed with an inverted logistic function avoiding background noise. Segmentation: StarDist2D over each 2D z-stack + Label Snitching (2D - > 3D Labels). Feature extraction: For each mask label we compute the volume, are extracted in voxels and then converted into microns using the metadata resolutions of the images. Analysis: Gausian Mixture Models (GMMs) to estimate a continuous Probability Density Function (PDF) of the volume in microns. Assessing the best GMM based on the Bayesian Information Criterion[26]. A statistic t-test was used for comparing groups.

### Statistical analysis

For comparisons of two groups, *t* test and Mann–Whitney tests were used. When data passed normality test, parametric *t* test was used when comparing two conditions and ANOVA for multiple comparisons. Non-parametric Mann–Whitney or Kruskall–Wallis' test were used for non-normal samples. In Fig. 1F, Kolmogoroff–Smirnoff test was employed to discern distribution differences by comparing cumulative distributions. p for binucleated is: 9.462586443476129e-06 and for the mononucleated: 0.002351632608523525. Raw numerical data available in FigShare https://doi.org/10.6084/m9.figshare.29108927. All comparisons (and graphs) were made using Prism9.0 from GraphPad.

### Reporting summary

Further information on research design is available in the Nature Portfolio Reporting Summary linked to this article.

## Data availability

Raw data supporting the findings generated in this study have been deposited in "FigShare" (Villa del Campo,2025) with the identifier https://doi.org/10.6084/m9.figshare.29108927.v3

Received: 25 October 2024; Accepted: 8 June 2025;
Published online: 18 July 2025

## References

1. Jessup, M. et al. *2009* focused update: ACCF/AHA Guidelines for the Diagnosis and Management of Heart Failure in Adults: a report of the American College of Cardiology Foundation/American Heart Association Task Force on Practice Guidelines: developed in collaboration with the International Society for Heart and Lung Transplantation. *Circulation,* **119**, 1977–2016 (2009).
2. Soonpaa, M. H. et al. Cardiomyocyte DNA synthesis and binucleation during murine development. *Am. J. Physiol.* **2712**, H2183–H2189 (1996).
3. Senyo, S. E. et al. Mammalian heart renewal by pre-existing cardiomyocytes. *Nature* **493**, 433–436 (2013).
4. Porrello, E. R. et al. MiR-15 family regulates postnatal mitotic arrest of cardiomyocytes. *Circ. Res.* **109**, 670–679 (2011).
5. Porrello, E. R. et al. Transient regenerative potential of the neonatal mouse heart. *Science* **331**, 1078–1080 (2011).
6. Poss, K. D., Wilson, L. G. & Keating, M. T. Heart regeneration in zebrafish. *Science* **298**, 2188–2190 (2002).
7. Bergmann, O. et al. Evidence for cardiomyocyte renewal in humans. *Science* **324**, 98–102 (2009).
8. Leone, M. & Engel, F. B. Pseudo-bipolar spindle formation and cell division in postnatal binucleated cardiomyocytes. *J. Mol. Cell Cardiol.* **134**, 69–73 (2019).
9. Gan, P., Patterson, M. & Sucov, H. M. Cardiomyocyte Polyploidy and Implications for Heart Regeneration. *Annu Rev. Physiol.* **82**, 45–61 (2020).
10. Patterson, M. et al. Frequency of mononuclear diploid cardiomyocytes underlies natural variation in heart regeneration. *Nat. Genet* **49**, 1346–1353 (2017).
11. Gonzalez-Rosa, J. M. et al. Myocardial Polyploidization Creates a Barrier to Heart Regeneration in Zebrafish. *Dev. Cell* **44**, 433–446.e7 (2018).
12. Shen, H. et al. Mononuclear diploid cardiomyocytes support neonatal mouse heart regeneration in response to paracrine IGF2 signaling. *Elife* **9** (2020).
13. Munoz-Martin, N. et al. Myc is dispensable for cardiomyocyte development but rescues Mycn-deficient hearts through functional replacement and cell competition. *Development* **146** (2019).
14. Bywater, M. J. et al. Reactivation of Myc transcription in the mouse heart unlocks its proliferative capacity. *Nat. Commun.* **11**, 1827 (2020).
15. Xiao, G. et al. Inducible activation of c-Myc in adult myocardium in vivo provokes cardiac myocyte hypertrophy and reactivation of DNA synthesis. *Circ. Res.* **89**, 1122–1129 (2001).
16. Ahuja, P. et al. Myc controls transcriptional regulation of cardiac metabolism and mitochondrial biogenesis in response to pathological stress in mice. *J. Clin. Invest* **120**, 1494–1505 (2010).
17. Jackson, T. et al. The c-myc proto-oncogene regulates cardiac development in transgenic mice. *Mol. Cell Biol.* **10**, 3709–3716 (1990).
18. Robbins, R. J. & Swain, J. L. C-myc protooncogene modulates cardiac hypertrophic growth in transgenic mice. *Am. J. Physiol.* **262**, H590–H597 (1992).
19. Zhong, W. et al. Hypertrophic growth in cardiac myocytes is mediated by Myc through a Cyclin D2-dependent pathway. *EMBO J.* **25**, 3869–3879 (2006).
20. Villa Del Campo, C. et al. Cell competition promotes phenotypically silent cardiomyocyte replacement in the mammalian heart. *Cell Rep.* **8**, 1741–1751 (2014).
21. Claveria, C. et al. Myc-driven endogenous cell competition in the early mammalian embryo. *Nature* **500**, 39–44 (2013).
22. Agah, R. et al. Gene recombination in postmitotic cells. Targeted expression of Cre recombinase provokes cardiac-restricted, site-specific rearrangement in adult ventricular muscle in vivo. *J. Clin. Invest* **100**, 169–179 (1997).
23. Yao, Z. et al. Identifying Cardiomyocyte Ploidy With Nuclear Area and Volume. *Circulation* **149**, 1540–1542 (2024).
24. Xiao, G. et al. Inducible activation of c-Myc in adult myocardium in vivo provokes cardiac myocyte hypertrophy and reactivation of DNA synthesis. *Circulation Res.* **89**, 1122–1129 (2001).
25. Cruz-Adalia, A. et al. CD69 limits the severity of cardiomyopathy after autoimmune myocarditis. *Circulation* **122**, 1396–1404 (2010).
26. DeLaughter, D. M. et al. Single-Cell Resolution of Temporal Gene Expression during Heart Development. *Dev. Cell* **39**, 480–490 (2016).

## Acknowledgements

The authors thank members of the Torres group for helpful comments and discussions and the CNIC personnel of the Microscopy and Compared Medicine Units for their support to this work. Biomedical Imaging has been conducted at the Advanced Imaging Unit of the CNIC. This work was supported by the European Commission H2020 Program grant SC1-BHC-

07-2019. Ref. 874764 “REANIMA” to M.T.; the Spanish Ministerio de Ciencia e Innovación grant PGC2018-096486-B-I00 to M.T.; Grant TNE-17CVD04 from the Leducq Foundation to M.T.; Comunidad de Madrid grant P2022/BMD-7245 to M.T.; ERC AdG REACTIVA Ref. 101142005 For experiments in the Unidad de Microscopía e Imagen Dinámica, CNIC, ICTS-ReDib, MCIN/AEI /10.13039/501100011033 and FEDER “Una manera de hacer Europa” (#ICTS-2018-04-CNIC-16). JPP received the support of a fellowship from”la Caixa” Foundation (ID 100010434). The fellowship code is LCF/BQ/DR22/11950017”. The CNIC is supported by the Ministerio de Ciencia e Innovación and the Pro CNIC Foundation and is a Severo Ochoa Center of Excellence (Grant number CEX2020-001041-S, funded by MICIU/AEI 10.13039/501100011033).

## Author contributions

C.V. dC., Conceptualization, Methodology, Formal Analysis, Investigation, Visualization, Writing-Original Draft, Writing-Review and Editing. M.R. and I.M. Image and Bioinformatics analysis of CM ploidy. R.S., I.E., and J.P., Methodology; M.T. Conceptualization, Writing-Review and Editing, Supervision, Funding Acquisition.

## Competing interests

The authors declare no competing interests

## Additional information

**Supplementary information** The online version contains supplementary material available at https://doi.org/10.1038/s42003-025-08360-w.

**Correspondence** and requests for materials should be addressed to Cristina Villa del Campo or Miguel Torres.

**Peer review information** *Communications Biology* thanks Eldad Tzahor and the other, anonymous, reviewer(s) for their contribution to the peer review of this work. Primary Handling Editor: Dario Ummarino. A peer review file is available.

**Reprints and permissions information** is available at http://www.nature.com/reprints

**Publisher’s note** Springer Nature remains neutral with regard to jurisdictional claims in published maps and institutional affiliations.

**Open Access** This article is licensed under a Creative Commons Attribution-NonCommercial-NoDerivatives 4.0 International License, which permits any non-commercial use, sharing, distribution and reproduction in any medium or format, as long as you give appropriate credit to the original author(s) and the source, provide a link to the Creative Commons licence, and indicate if you modified the licensed material. You do not have permission under this licence to share adapted material derived from this article or parts of it. The images or other third party material in this article are included in the article’s Creative Commons licence, unless indicated otherwise in a credit line to the material. If material is not included in the article’s Creative Commons licence and your intended use is not permitted by statutory regulation or exceeds the permitted use, you will need to obtain permission directly from the copyright holder. To view a copy of this licence, visit http://creativecommons.org/licenses/by-nc-nd/4.0/.

© The Author(s) 2025